

Stable Cosmic Vortons

Julien Garaud,^{1,2} Eugen Radu,³ and Mikhail S. Volkov⁴

¹*Department of Physics, University of Massachusetts Amherst, MA 01003 USA.*

²*Department of Theoretical Physics, The Royal Institute of Technology, Stockholm, SE-10691 SWEDEN.*

³*Institut für Physik, Universität Oldenburg, Postfach 2503 D-26111 Oldenburg, GERMANY.*

⁴*Laboratoire de Mathématiques et Physique Théorique CNRS-UMR 7350, Université de Tours, Parc de Grandmont, 37200 Tours, FRANCE.*

(Dated: March 14, 2013)

We present for the first time solutions in the gauged $U(1) \times U(1)$ model of Witten describing vortons – spinning flux loops stabilized against contraction by the centrifugal force. Vortons were heuristically described many years ago, however, the corresponding field theory solutions were not obtained and so the stability issue remained open. We construct explicitly a family of stationary vortons characterized by their charge and angular momentum. Most of them are unstable and break in pieces when perturbed. However, thick vortons with small radius preserve their form in the $3 + 1$ non-linear dynamical evolution. This gives the first ever evidence of stable vortons and impacts several branches of physics where they could potentially exist. These range from cosmology, where vortons could perhaps account for the cold dark matter, to condensed matter physics.

PACS numbers: 11.10.Lm, 11.27.+d, 98.80.Cq

More than 25 years ago Witten introduced the idea of superconducting cosmic strings in the context of a field theory model that can be viewed as a sector of a Grand Unification Theory (GUT) [1]. The model admits classical solutions describing strings (vortices) whose longitudinal current can attain astronomical values, implying interesting effects (see [2] for a review).

Soon after, it was realized that superconducting strings could form loops whose current would produce an angular momentum supporting them against contraction [3]. If stable, such cosmic vortons should be of considerable physical interest. However, until very recently it was not clear if vortons are stable or not, since the underlying field theory solutions were not known. Various approximations were used to describe vortons, for example, by viewing them as thin and large elastic rings [4]. At the same time, it was realized that objects similar to vortons could potentially exist also in other branches of physics, as for example in condensed matter physics [5], or in QCD [6]. Since superconducting strings exist in the Weinberg-Salam theory [7], vortons are potentially possible also there.

The first field theory solutions describing stationary vortons were found in the global limit of Witten's model, when the gauge fields vanish [8]. These vortons have approximately equal radius and thickness and remind a Horn torus. Solutions describing thin and large vortons were later found as well, however, when perturbed, thin vortons turn out to be dynamically unstable and break in pieces [9]. Although discouraging, this result is actually quite natural, since thin vortons can be locally approximated by straight strings, while the latter are known to become unstable for large currents [2].

However, a more close inspection reveals that unstable modes of superconducting strings have a non-zero minimal wavelength [10], as in the case of the Plateau-Rayleigh instability of a water jet [11]. Therefore, imposing periodic boundary conditions with a short enough period should remove all

instabilities. As a result, thick vortons made of short string pieces have chances to be stable.

In this letter we present for the first time stationary vorton solutions in the gauged Witten's model, and our vortons are thick. To study their stability, we simulate their full $3 + 1$ non-linear dynamics in the limit of vanishing gauge couplings. We find that most of them are unstable, however, thick vortons with a large charge and the smallest possible radius are stable. By continuity, it follows that vortons with non-zero but small gauge couplings should be stable as well.

We therefore present the first evidence of stable vortons, whose features turn out to be quite different from those predicted by the effective theories. This can impact several branches of physics where vortons could potentially exist, ranging from cosmology and high energy physics to condensed matter physics.

The model of Witten.– This is a theory of two Abelian vectors $A_\mu^{(a)}$ interacting with two complex scalars Φ_a ($a = 1, 2$) with the Lagrangian

$$\mathcal{L} = -\frac{1}{4} \sum_a F_{\mu\nu}^{(a)} F^{(a)\mu\nu} + \sum_a (D_\mu \Phi_a)^* D^\mu \Phi_a - V. \quad (1)$$

Here the gauge field strengths are $F_{\mu\nu}^{(a)} = \partial_\mu A_\nu^{(a)} - \partial_\nu A_\mu^{(a)}$, the gauge covariant derivatives $D_\mu \Phi_a = (\partial_\mu + ig_a A_\mu^{(a)}) \Phi_a$ with gauge couplings g_a , and the potential is

$$V = \sum_a \frac{\lambda_a}{4} (|\Phi_a|^2 - \eta_a^2)^2 + \gamma |\Phi_1|^2 |\Phi_2|^2 - \frac{\lambda_2 \eta_2^4}{4}, \quad (2)$$

where $\eta_1 = 1$. If $4\gamma^2 > \lambda_1 \lambda_2$ and $2\gamma > \lambda_2 \eta_2^2$ then the global minimum of the potential (vacuum) is achieved for $|\Phi_1| = 1$ and $\Phi_2 = 0$. Fields $A_\mu^{(1)}$, Φ_1 , Φ_2 are massive with masses, respectively, $m_A^2 = 2g_1^2$, $m_1^2 = \lambda_1$, $m_2^2 = \gamma - \frac{1}{2} \lambda_2 \eta_2^2$ whereas $A_\mu^{(2)}$ is massless and can be identified with electromagnetic field. The theory has a local $U(1) \times U(1)$ invariance and two

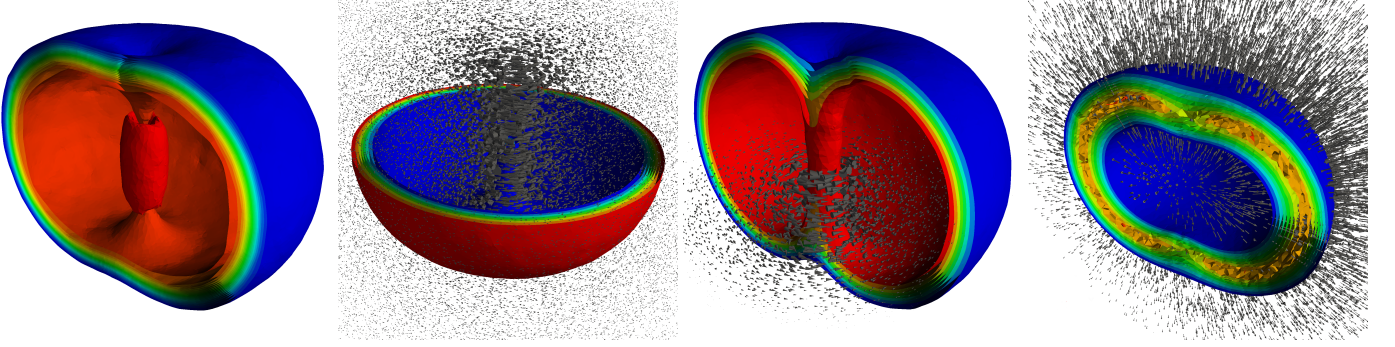


Figure 1. (Color online) – Profiles of the stationary vorton solution for $Q = 1500$ and $n = 1, m = 1$ for the parameter values $\lambda_1 = 41.1$, $(\lambda_2, \eta_2) = (30, 1)$, $\gamma = 20$, and $g_1 = g_2 = 0.01$. The configuration is very compact and close to a Horn torus. The first panel displays constant energy surfaces. The second panel shows surfaces of constant $|\Phi_1|^2$ and the magnetic field $\vec{B}^{(1)}$ (cones). One has $\vec{E}^{(1)} = 0$. The third panel shows $|\Phi_2|^2$ isosurfaces and the electromagnetic current \vec{j}_2 (cones). The last panel shows the electric field $\vec{E}^{(2)}$ (cones), while the isosurfaces show its magnitude. The red color corresponds to large values and the blue color to small values.

Noether currents, $j_a^\mu = 2\text{Re}(i\Phi_a^* D^\mu \Phi_a)$, with two conserved charges $\int j_a^t d^3x$. The Euler-Lagrange equations are

$$\partial_\mu F^{(a)\mu\nu} = g_a j_a^\nu, \quad D_\mu D^\mu \Phi_a + \frac{\partial V}{\partial |\Phi_a|^2} \Phi_a = 0. \quad (3)$$

Assuming cylindrical coordinates $x^\mu = (t, \rho, z, \varphi)$, we make the ansatz for stationary, axially symmetric fields,

$$\Phi_1 = X_1 + iY_1, \quad \Phi_2 = (X_2 + iY_2) \exp\{i(\omega t + m\varphi)\}, \quad (4)$$

where X_a, Y_a as well as $A_\mu^{(a)}$ depend on ρ, z , and we impose the gauge condition $A_\rho^{(a)} = 0$. Here m is an integer winding number and ω is a frequency. The fields should be globally regular and the energy should be finite, which requires that at infinity $X_1 \rightarrow 1$ while all other amplitudes approach zero. At the symmetry axis, $\rho = 0$, the amplitudes $X_2, Y_2, A_\varphi^{(a)}$ vanish, while for the other amplitudes the normal derivative $\partial/\partial\rho$ vanishes. Under the reflection $z \rightarrow -z$ the amplitudes Y_a are odd whereas all the others are even.

The choice of the ansatz implies that the first Noether charge vanishes, while the second one is

$$Q = 2 \int d^3x (X_2^2 + Y_2^2) (\omega - g_2 A_t^{(2)}). \quad (5)$$

The energy is $E = \int T_t^t d^3x$ and the angular momentum

$$J = \int T_\varphi^\varphi d^3x = mQ, \quad (6)$$

where the energy-momentum tensor is obtained by varying the metric tensor, $T_\nu^\mu = 2g^{\mu\sigma} \partial \mathcal{L} / \partial g^{\sigma\nu} - \delta_\nu^\mu \mathcal{L}$. In the above formulas all fields and coordinates are dimensionless. If η is the energy scale, then the dimensionful (boldfaced) quantities are $\Phi_a = \eta \Phi_a$, $A_\mu^{(a)} = \eta A_\mu^{(a)}$, $x^\mu = \mathbf{x}^\mu \eta$, $\mathbf{E} = \eta E$, hence η is the asymptotic value of Φ_1 .

Stationary vortons.— Inserting the ansatz (4) to the field equations (3) gives, after separating t and φ variables, an elliptic system of 10 non-linear PDE's for the 10 functions of

ρ, z . We solve these equations with two different numerical methods: using the elliptic PDE solver FIDISOL based on the Newton-Raphson procedure [12], and also minimizing the energy within a finite element approach provided by the Freefem++ library [13].

The resulting vorton solutions have a toroidal symmetry, with non-trivial windings along both torus generators. Apart from the azimuthal winding number m , there is a second integer, n , determining the winding of phase of Φ_1 around the boundary of the (ρ, z) half-plane. If $n \neq 0$ then Φ_1 vanishes at a point $(\rho_0, 0)$ corresponding to the center of the closed vortex forming the vorton, and the phase of Φ_1 winds around this point. We have constructed vortons for $n = 0, 1, 2$ and $m = 0, \dots, 12$. Solutions for $n = m = 0$ are spherically symmetric, they have $J = 0$ and are similar to Q-balls [14].

The vorton can be visualized as a toroidal tube confining a magnetic flux of $\vec{B}^{(1)} = \vec{\nabla} \times \vec{A}^{(1)}$ since $\Phi_1 \approx 0$ inside the tube and thus the first U(1) is restored. $\Phi^{(2)}$ is non-zero inside the tube, giving rise to a charged condensate and to a persistent electric current along the tube. The current creates a momentum along the azimuthal direction, which gives rise to an angular momentum along z -direction. Outside the vorton tube the massive fields $A_\mu^{(1)}, \Phi_1, \Phi_2$ rapidly approach their vacuum values and there remains only the long-range massless $A_\mu^{(2)}$ generated by the electric current confined inside the vorton tube. At large $r = \sqrt{\rho^2 + z^2}$ one has $A_t^{(2)} = Q/(4\pi r) + \dots$ and $A_\varphi^{(2)} = \mu \sin \theta / r^2 + \dots$, therefore, from far away the vorton looks like a superposition of an electric charge Q with a magnetic dipole μ .

Fig. 1 shows the 3D solution profiles for an $m = 1$ vorton. One can see that the vorton tube is very thick and compact. The vortex magnetic field $\vec{B}^{(1)} = \vec{\nabla} \times \vec{A}^{(1)}$ and the electric current \vec{j}_2 are tangent to the azimuthal lines. The electric field $\vec{E}^{(2)} = -\vec{\nabla} A_t^{(2)}$ is mostly oriented along the radial direction and supports a non-zero flux at infinity, $Q = \oint d\vec{E}^{(2)} \cdot d\vec{S} = g_2 Q$. The massless magnetic field $\vec{B}^{(2)} = \vec{\nabla} \times \vec{A}^{(2)}$ at large r is of magnetic dipole type.

Vortons can be labeled by their charge Q and the integer ‘spin’ $m = J/Q$ (assuming that $n = 1$). The vorton radius ρ_0 is not very sensitive to the value of Q but increases rapidly with m , so that for large m vortons are thin and large, with the radius much larger than the thickness. On the other hand, increasing Q increases the thickness of the vorton tube, so that for large Q vortons are thick and look almost spherical.

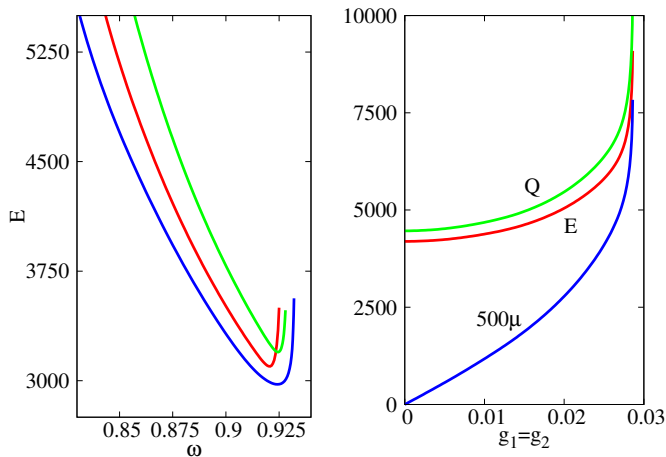


Figure 2. (Color online) – Left panel shows E against ω for the values of gauge couplings $(g_1, g_2) = (0.08, 0.02)$ (blue), $(0.01, 0.01)$ (red), $(0.08, 0.02)$ (green). Right panel shows E , Q , μ against $g_1 = g_2$ for a fixed $\omega = 0.804$. In both cases $\lambda_1 = 41.1$, $\lambda_2 = 40$, $\gamma = 22.3$, $\eta_2 = 1$, $n = 1$, $m = 2$.

The frequency ω can be used instead of Q to characterize the solutions, which exist only within a finite frequency range, $\omega_- < \omega < \omega_+$. Both E and Q diverge for $\omega \rightarrow \omega_{\pm}$ and have a minimum in between, as shown in Fig. 2. Vortons can be viewed as boson condensates, which is why their charge cannot be too small, since the boson condensation is not energetically favored for small quantities of the field quanta. For solutions with large Q and ω close to ω_- the value of E/Q is less than for free particles, therefore they cannot disintegrate into particles. In addition, for these solutions one has $E(m) < mE(m = 1)$, so that $m > 1$ vortons cannot disintegrate into $m = 1$ vortons. However, the possibility of disintegrating into Q-balls with $n = m = 0$ is not excluded.

In the limit of vanishing gauge coupling constants g_a the gauge fields vanish and the solutions reduce to global vortons obtained in [8]. These can be visualized as closed tubes inside which $\Phi_1 \approx 0$ but Φ_2 is non-zero and creates the global azimuthal current, while outside $\Phi_1 \approx 1$ and $\Phi_2 \approx 0$. For $g_a \neq 0$ the gauge fields are excited and increase the total energy and charge, as shown in Fig. 2.

We find that solutions do not exist for arbitrary values of the model parameters λ_a , η_2 , γ , g_a but only for some regions in the parameter space. For example, fixing all parameters and also ω and varying $g_1 = g_2$, the solutions exist only within a finite range of gauge couplings, as is seen in Fig. 2.

Dynamical vortons.– The key question is the vorton stability, and we therefore analyze their non-linear $3 + 1$ dynam-

ics. In doing this, we consider only the global vortons without gauge fields, since simulating dynamics of the fully gauged vortons would require too much computer power. However, we expect the results obtained in the global case to apply to the fully gauged vortons as well, at least for small enough gauge couplings g_a . Indeed, if $g_a = 0$ then the vorton is made of two scalars Φ_a with global currents $j_a^\nu(\Phi_a)$. For $g_a \neq 0$ the currents give rise to the source $g_a j_a^\nu$ in the gauge field equations (3), hence for small g_a one will have $A_\mu^{(a)} \sim g_a$. The backreaction of the gauge fields on the scalars will be then proportional to g_a^2 and can be neglected as compared to the reaction of the scalars on themselves. As a result, the gauged vortons for small g_a are essentially global vortons and the gauge field dynamics can be neglected. This is confirmed by the numerics, as can be seen in the right panel of Fig. 2.

The dynamical evolution of global vortons was previously studied in [9] for large ‘spins’ m , when vortons are thin and large. It was found that when perturbed, the vortons rapidly develop pinching deformations which break them in pieces. This is quite natural, since thin and long vortons can be locally approximated by straight vortex pieces, but the latter are known to be unstable, unless they are so short that there is no room for the instability to settle in [10]. Therefore, to get rid of instabilities one has to ‘make vortons’ of as short vortex pieces as possible, in which case the vorton radius would be the smallest. In other words, the ‘spin’ m should be small.

To verify this conjecture, we considered a hyperbolic evolution scheme based on an implicit β -Newmark finite difference approximation. The space dependence is implemented within a finite element method providing a triangulation of a spherical volume in 3-space. At the boundary of the volume the fields are held at their vacuum values, which insures the absence of outgoing radiation (details of our numerical method are given in the Appendix). The initial configuration is a stationary, axially symmetric vorton solution. This configuration becomes automatically perturbed by the space discretization, and this triggers a non-trivial temporal evolution.

The natural timescale is set by the value of ω of the underlying vorton solution, which is of order one, and so one can choose the timescale to be one. We then integrate with the timestep $\Delta t = 0.1$ and find that the $m \geq 3$ vortons very quickly become strongly deformed and then break in pieces. The time they take to break decreases rapidly as the ‘spin’ grows. For example, the $m = 6$ solution shown in Fig. 3 breaks already for $t \approx 20$, while the one with $m = 3$ survives till $t \approx 40$ (see [15] for the online videos).

The products of the vorton decay are typically two or more out-spirling fragments of spherical topology (Q-balls) carrying fractions of the initial Noether charge. The angular momentum of the initial vorton transforms into the orbital angular momenta of the fragments. The number of fragments depends on the initial charge and angular momentum.

We therefore conclude that thin and large vortons are unstable, thus confirming the result of [9]. One should say that a different conclusion was previously made in Ref. [16], where thin vortons were found to be stable. Since neither our anal-

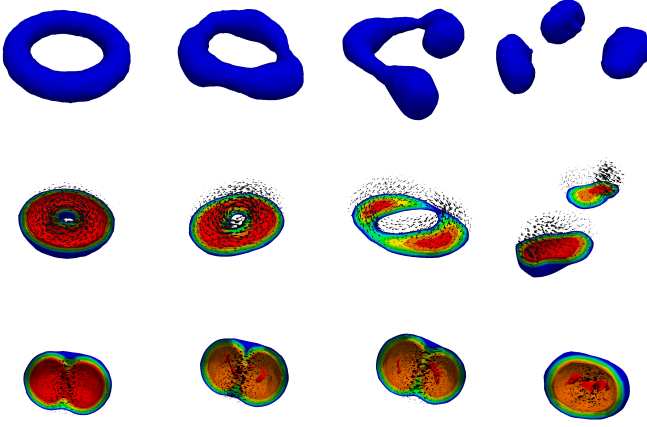


Figure 3. (Color online) – Snapshots of the vorton time evolution. The first line shows a constant $|\Phi_2|^2$ surface for the $m = 6$ solution for $t = 0, 17, 21, 28$. The second and third lines show the constant $|\Phi_1|^2$ surfaces and the electric current, respectively, for $m = 3$ vorton for $t = 0, 31, 28, 47$ and for the $m = 1$ vorton for $t = 0, 104, 153, 239$. The third line shows the stable solution for $Q = 6000$ and for the same values of $\lambda_a, \eta_2, \gamma$ as in Fig. 2.

ysis nor that of [9] confirm this, it is possible that the conclusion of [16] is an artifact of modifying the scalar potential made in that work in order to improve the stability behavior. The authors of [16] also admit that their results are extremely sensitive to the initial conditions (unlike in our case), hence it is possible that they find some long-living metastable states.

We finally turn to vortons with $m = 1, 2$ and choose a large value Q , in which case the vortons are compact and thick. For $m = 2$ we cannot make a definite conclusion, since the vortons do not actually break but sometimes become strongly deformed. Although each time they manage to restore their original shape, it is not excluded that they will break in the long run.

However, nothing at all happens to the $m = 1$ vortons. As the time goes, they only move slowly in the box, sometimes reflecting from the boundary, without any visible change of shape. We integrated up to $t \sim 10^3$ (which requires weeks of runtime) without noticing any change in their behavior. We also checked that increasing the size of the box does not change anything, so that one cannot say that the boundary has a stabilizing effect. We therefore conclude that vortons with the lowest ‘spin’ and a large enough charge are stable. Intuitively, this is because they are so thick that they are ‘hard to pinch’.

Interestingly, a very similar conclusion was made for the ‘spinning light bullets’ which share many properties with vortons [17]. These are non-relativistic solutions for a complex scalar field with a t, φ -dependent phase (like for Φ_2), and they also have toroidal profiles. The profile of their energy $E(\omega)$ is similar to that shown in Fig. 2. It was found that the $m = 1$ solutions with a large charge and ω close to ω_- preserve their

shape in the $3 + 1$ dynamical evolution [17]. Exactly the same statement applies for our relativistic vortons.

In summary, for the first time since the vortons were heuristically described almost 25 year ago [3], we present the underlying stable solutions within the $U(1) \times U(1)$ gauge field theory of Witten [1]. These vortons are quite different from what was expected before – instead of being thin and large rings, they look like thick doughnuts of almost spherical shape.

We can now make some estimates. Assuming the original motivation of Witten, the energy scale should be of the GUT magnitude, $\eta \sim 10^{14}$ GeV. Using the value $E \sim 5 \times 10^3$ for estimates (see Fig. 2), it follows that vortons are very small and extremely heavy, with $E \sim 5 \times 10^{17}$ GeV, which is not far from the Planck energy. If some versions of GUTs containing a $U(1) \times U(1)$ sector indeed applied in the past and the vortons have survived till present, then they could perhaps account for the non-relativistic cold dark matter. Since g_2 can be small or vanish, the vorton electric field is not necessarily very large.

For $g_a = 0$ and stationary fields Eq.(3) can formally be interpreted as the non-relativistic Gross-Pitaevskii equation for a two-component Bose-Einstein condensate (BEC) [8]. Therefore, our solutions describe also vortex loops in BECs. Equally, Eq.(3) can be viewed as describing a condensate of K -mesons in QCD, hence our solutions describe the K -vortons, whose existence was conjectured in [6]. Setting the scale to be $\eta \sim 200$ MeV gives for their energy $E \sim 1$ TeV. Although in each particular case one has to adjust the parameters to the physical values, the conclusion is that the existence of stable vortons impacts several branches of physics.

J.G. was supported by the NSF grant No. DMR-0955902 and by the Swedish Research Council. A part of this work was performed at the Royal Institute of Technology, Sweden on resources provided by the Swedish National Infrastructure for Computing at the National Supercomputer Center in Linköping, Sweden. E.R. gratefully acknowledges support by the DFG.

-
- [1] E. Witten, *Nucl. Phys.* **B249**, 557 (1985)
 - [2] A. Vilenkin and E. Shellard, *Cosmic Strings and Other Topological Defects* (Cambridge University Press, 2000) ISBN 9780521654760
 - [3] R. L. Davis and E. P. S. Shellard, *Nucl. Phys.* **B323**, 209 (1989)
 - [4] B. Carter, *Phys.Lett.* **B238**, 166 (1990)
 - [5] R. A. Battye, N. R. Cooper, and P. M. Sutcliffe, *Phys. Rev. Lett.* **88**, 080401 (2002) E. Babaev, *ibid.* **88**, 177002 (2002) C. M. Savage and J. Ruostekoski, *ibid.* **91**, 010403 (2003) M. A. Metlitski and A. R. Zhitnitsky, *JHEP* **06**, 017 (2004) M. Nitta, K. Kasamatsu, M. Tsubota, and H. Takeuchi, *Phys. Rev. A* **85**, 053639 (May 2012)
 - [6] K. B. Buckley, M. A. Metlitski, and A. R. Zhitnitsky, *Phys.Rev.* **D68**, 105006 (2003)
 - [7] J. Garaud and M. S. Volkov, *Nucl. Phys.* **B826**, 174 (2010)
 - [8] E. Radu and M. S. Volkov, *Phys. Rept.* **468**, 101 (2008)
 - [9] R. A. Battye and P. M. Sutcliffe, *Nucl. Phys.* **B814**, 180 (2009)
 - [10] J. Garaud and M. S. Volkov, *Nucl. Phys.* **B839**, 310

(2010) **B799**, 430 (2008)

- [11] J. Eggers, *Rev. Mod. Phys.* **69**, 865 (Jul 1997)
- [12] W. Schönauer and E. Schnepf, *ACM Trans. Math. Softw.* **13**, 333 (1987)
- [13] F. Hecht, O. Pironneau, A. Le Hyaric, and K. Ohtsuka, *The Freefem++ manual* (2007) www.freefem.org
- [14] K.-M. Lee, J. A. Stein-Schabes, R. Watkins, and L. M. Widrow, *Phys. Rev. D* **39**, 1665 (1989)
- [15] Videos of the dynamical evolution of vortons are available online at <http://people.umass.edu/garaud/Webpage/vortons.html>
- [16] Y. Lemperiere and E. P. S. Shellard, *Phys. Rev. Lett.* **91**, 141601 (2003)
- [17] D. Mihalache, D. Mazilu, L.-C. Crasovan, I. Towers, A. V. Buryak, B. A. Malomed, L. Torner, J. P. Torres, and F. Lederer, *Phys. Rev. Lett.* **88**, 073902 (Feb 2002)

APPENDIX. NUMERICAL DETAILS

We used three completely different numerical techniques for the vorton construction. First, we performed our calculations using the elliptic PDE solver FIDISOL based on the iterative Newton-Raphson method [12] within a finite difference scheme. This method was used to solve the equations (3) for the stationary, axially symmetric fields (4). Next, we re-

produced the same solutions using the energy minimization scheme within a finite element framework provided by the Freefem++ library [13]. Finally, we simulated the hyperbolic evolution of the full 3 + 1 theory, also using the Freefem++ library [13]. Below we shall describe the two last methods.

Energy minimization

The energy-momentum tensor of Witten's model (1) is

$$T_{\nu}^{\mu} = - \sum_a F^{(a)\mu\rho} F_{\nu\rho}^{(a)} + \sum_a (D^{\mu}\Phi_a)^* D_{\nu}\Phi_a + \sum_a (D_{\nu}\Phi_a)^* D^{\mu}\Phi_a - \delta_{\nu}^{\mu} \mathcal{L}, \quad (\text{A.1})$$

and the energy $E = \int T_t^t d^3x$. Using the axially symmetric ansatz in the radial gauge,

$$A_{\mu}^{(a)} dx^{\mu} = V^{(a)} dt + W^{(a)} d\varphi + Z^{(a)} dz, \quad (\text{A.2})$$

$$\Phi_1 = X_1 + iY_1, \Phi_2 = (X_2 + iY_2) \exp\{i(\omega t + m\varphi)\},$$

where $X_a, Y_a, V^{(a)}, W^{(a)}, Z^{(a)}$ depend on ρ, z , gives

$$E = \int \left\{ \frac{1}{2} \sum_a \left(\nabla V^{(a)2} + \frac{1}{\rho^2} \nabla W^{(a)2} + \partial_{\rho} Z^{(a)2} \right) + 2 \sum_a g_a Z^{(a)} (Y_a \partial_z X_a - X_a \partial_z Y_a) + \nabla X_1^2 + \nabla Y_1^2 + \nabla X_2^2 + \nabla Y_2^2 + \left((g_1 V^{(1)})^2 + \left(\frac{g_1}{\rho} W^{(1)} \right)^2 + (g_1 Z^{(1)})^2 \right) (X_1^2 + Y_1^2) + \frac{\lambda_1}{4} (X_1^2 + Y_1^2 - \eta_1^2)^2 + \gamma (X_1^2 + Y_1^2) (X_2^2 + Y_2^2) + \left((\omega - g_2 V^{(2)})^2 + \frac{1}{\rho^2} (m - g_2 W^{(2)})^2 + (g_2 Z^{(2)})^2 + \frac{\lambda_2}{4} (X_2^2 + Y_2^2 - 2\eta_2^2) \right) (X_2^2 + Y_2^2) \right\} d^3x, \quad (\text{A.3})$$

where $\nabla \equiv (\partial_{\rho}, \partial_z)$ denotes the gradient operator in the (ρ, z) -plane. We find stationary solutions by minimizing the energy for a fixed Noether charge. To this end, we express the frequency ω in terms of Q via rewriting Eq. (5) in the form

$$Q = 2(\omega \Sigma_1 - \Sigma_2) \quad (\text{A.4})$$

with

$$\begin{aligned} \Sigma_1 &= \int d^3x (X_2^2 + Y_2^2), \\ \Sigma_2 &= \int d^3x g_2 V^{(2)} (X_2^2 + Y_2^2), \end{aligned} \quad (\text{A.5})$$

so that

$$\omega = \frac{Q + 2\Sigma_2}{2\Sigma_1}, \quad (\text{A.6})$$

which should be inserted to (A.3). The energy is then minimized at a fixed Q .

Since the integrand in (A.3) does not depend on φ and is invariant under $z \rightarrow -z$, we choose the integration domain to be a quadrant of radius r_{\max} ,

$$\Omega := \left\{ \rho, z \in [0, r_{\max}] \times [0, r_{\max}] \mid \sqrt{\rho^2 + z^2} \leq r_{\max} \right\}, \quad (\text{A.7})$$

this is illustrated in Fig. 4. Regularity conditions at the symmetry axis require that at $\rho = 0$ one has

$$\begin{aligned} X_2 &= Y_2 = 0, \partial_{\rho} X_1 = \partial_{\rho} Y_1 = 0, \\ W^{(a)} &= 0, \partial_{\rho} V^{(a)} = \partial_{\rho} Z^{(a)} = 0. \end{aligned} \quad (\text{A.8})$$

The reflexion symmetry in the equatorial plane implies that at $z = 0$

$$\begin{aligned} \partial_z X_a &= 0, Y_a = 0, \\ \partial_z V^{(a)} &= \partial_z W^{(a)} = \partial_z Z^{(a)} = 0. \end{aligned} \quad (\text{A.9})$$

Since the massive fields approach their asymptotic values exponentially fast, we assume that for $\sqrt{\rho^2 + z^2} = r_{\max}$ the

fields take on the vacuum values

$$X_1 = 1, Y_1 = X_2 = Y_2 = 0, \quad \text{and} \quad A_\mu^{(a)} = 0, \quad (\text{A.10})$$

but then we refine this by imposing mixed boundary conditions for the massless $A_\mu^{(2)}$ to take into account its slow falloff.

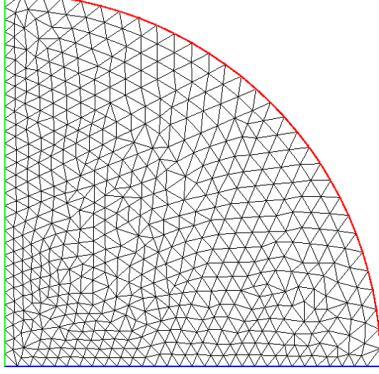


Figure 4. (Color online) – Triangulation over the computational domain.

The variational problem of minimizing (A.3) is defined for numerical computations by adapting a finite element formulation provided by the Freefem++ library [13]. The discretization within this formulation is done via a (homogeneous) triangulation over Ω , based on the Delaunay-Voronoi algorithm (see Fig. 4). The functions are expanded with respect to a continuous piecewise quadratic polynomial basis on each triangle. The accuracy of the method is controlled by the number of triangles, by the order of expansion in the basis for each triangle, and also by the order of the quadrature formula for the integral over the triangles. Once the problem is mathematically posed, a numerical optimization algorithm is used to solve the nonlinear variational problem of finding the minima of E . We used a nonlinear conjugate gradient method. The algorithm is iterated until the relative variation of the norm of the gradient of the functional E with respect to all degrees of freedom is less than 10^{-6} . Virial relations which should be fulfilled by the solutions are then checked.

Hyperbolic evolution

To investigate the dynamical stability of the global vortons, the axially symmetric solutions are used as the initial data for a $3 + 1$ evolution code. This time the integration domain Ω is an (open) bounded subset of \mathbb{R}^3 with the boundary $\partial\Omega$ and with the attached normal derivative ∂_n . We choose Ω to be the interior of a sphere of radius r_{\max} . The discrete version is obtained by a homogeneous triangulation over Ω . The following numerical scheme was used to evolve the vortons. The

dynamical equations for the scalars read in the global limit

$$\partial_{tt}\Phi_a - \Delta\Phi_a + \frac{\partial V}{\partial|\Phi_a|^2}\Phi_a = 0. \quad (\text{A.11})$$

Here $\Delta \equiv \vec{\nabla}^2$ is the Laplace operator and $\vec{\nabla}$ the gradient operator in three space dimensions in Cartesian coordinates. The weak formulation of the hyperbolic problem (A.11) is obtained by multiplying the equation by test functions w_a , integrating over Ω and applying the Stokes formula,

$$\begin{aligned} \int_{\Omega} w_a \partial_{tt}\Phi_a + \int_{\Omega} \vec{\nabla} w_a \cdot \vec{\nabla} \Phi_a + \int_{\Omega} w_a \frac{\partial V}{\partial|\Phi_a|^2} \Phi_a \\ - \int_{\partial\Omega} w_a \partial_n \Phi_a = 0. \end{aligned} \quad (\text{A.12})$$

The time discretization is achieved using a β -Newmark scheme, which converts (A.12) to

$$\begin{aligned} \int_{\Omega} w_a \frac{\Phi_a^{[n+1]} - 2\Phi_a^{[n]} + \Phi_a^{[n-1]}}{dt^2} \\ + \int_{\Omega} \vec{\nabla} w_a \cdot \vec{\nabla} \left(\beta\Phi_a^{[n+1]} + (1-2\beta)\Phi_a^{[n]} + \beta\Phi_a^{[n-1]} \right) \\ + \int_{\Omega} w_a \frac{\partial V^{[n]}}{\partial|\Phi_a|^2} \Phi_a^{[n]} - \int_{\partial\Omega} w_a \partial_n \Phi_a^{[n]} = 0, \end{aligned} \quad (\text{A.13})$$

where $\Phi_a^{[n]}, V^{[n]}$ are the value of Φ_a, V at the time moment $t_0 + ndt$. Here $0 \leq \beta \leq 1$ and the scheme is unconditionally stable for $\beta \geq 1/4$. Typically we choose $\beta = 1/4$, which corresponds to the constant average acceleration method, while choosing $\beta = 1/2$ would reproduce the Crank-Nicolson scheme. We assume that $\partial_t \Phi_a = 0$ at $\partial\Omega$, so that the boundary values of fields are frozen.

The time-discretized equations (A.13) can be rewritten as a recurrence

$$u^{[n+1]} = \mathbf{A}^{-1} \left(\mathbf{B}u^{[n]} + \mathbf{C} \right) - u^{[n-1]} \quad (\text{A.14})$$

where $u^{[n]} \equiv \{u_i^{[n]}\}$ is the vector containing all discretized degrees of freedom at the n -th time step. \mathbf{A}, \mathbf{B} are matrix bilinear operators and \mathbf{C} is a vector containing the nonlinearities,

$$\begin{aligned} \mathbf{A}_{ij} &= \int_{\Omega} (u_j^{[n]} u_i^{[n]} + \beta_1 \vec{\nabla} u_j^{[n]} \cdot \vec{\nabla} u_i^{[n]}) - \int_{\partial\Omega} \beta_1 u_j^{[n]} \partial_n u_i^{[n]}, \\ \mathbf{B}_{ij} &= \int_{\Omega} (2u_j^{[n]} u_i^{[n]} - \beta_2 \vec{\nabla} u_j^{[n]} \cdot \vec{\nabla} u_i^{[n]}) + \int_{\partial\Omega} \beta_2 u_j^{[n]} \partial_n u_i^{[n]}, \\ \mathbf{C}_i &= -dt^2 \int_{\Omega} u_i^{[n]} \frac{\partial V^{[n]}}{\partial|\Phi_a|^2} \Phi_a^{[n]}, \end{aligned} \quad (\text{A.15})$$

with $\beta_1 = \beta dt^2$ and $\beta_2 = (1-2\beta)dt^2$. Using the stationary, axially symmetric solutions obtained by minimizing the energy, the recurrence is initialized by

$$\begin{aligned} \Phi_1^0 &= X_1(\rho, |z|) + i \text{sg}(z) Y_1(\rho, |z|), & \Phi_1^1 &= \Phi_1^0 \\ \Phi_2^0 &= (X_2(\rho, |z|) + i \text{sg}(z) Y_2(\rho, |z|)) e^{im\varphi}, & \Phi_2^1 &= \Phi_2^0 e^{i\omega dt}. \end{aligned} \quad (\text{A.16})$$

The time step dt is typically chosen to be 0.1 and the configuration is evolved for several hundreds of internal periods $T = 2\pi/\omega$.